

#### **Original Article**

# Improving the dissolution rate of cilnidipine via nano-micellar formulation aided with *In-vitro* characterization and *Ex-vivo* permeation

Manar Adnan Tamer<sup>1</sup>, Maha Mahdi Ali<sup>2\*</sup>, Ishraq K. Abbas<sup>3</sup>, Mowafaq M. Ghareeb<sup>1</sup>

<sup>1</sup>Department of Pharmaceutics, College of Pharmacy, University of Baghdad, Baghdad, Iraq. <sup>2</sup>Department of Pharmaceutics, College of Pharmacy, University of Hilla, Babylon, Iraq. <sup>3</sup>Faculty of Pharmacy, Al-Rafidain University College, Baghdad, Iraq.

Correspondence: Maha Mahdi Ali, Department of Pharmaceutics, College of Pharmacy, University of Hilla, Babylon, Iraq. mahamahdiali@gmail.com

Received: 11 June 2025; Revised: 27 October 2025; Accepted: 29 October 2025

#### **ABSTRACT**

The goal of this study is to improve the oral bioavailability of Clindipine (CLD) by converting it into a nano-micellar (NM) dosage form, which will improve its dissolving rate. Nanocarriers such as Soluplus (SLP), D- $\alpha$ -tocopherol polyethylene glycol 1000 succinate (TPGS), Poloxamer (POL 188), and Tween-80 were used to prepare CLD as nano-micellar dispersion (CLD-NM) with one polymer in 1:2, 1:4, 1:6, and 1:8 ratios or with a polymer combination in 1:4:1 and 1:4:2 ratios using the thin film hydration method. Thirteen formulas were produced and principally tested for their physical stability. They were then tested for particle size (P size), polydispersity (PDI), entrapment efficiency (EE%), and drug loading (DL%), followed by in vitro and ex vivo tests. Only the selected formula was studied in terms of morphology and compatibility. The drug-loaded nano-micelles of the selected formula coded (F12) were analyzed and determined to be: micelle size (43.76±0.3 nm), PDI (0.2899±0.02), EE% (99.99±0.2%), and DL% (16.7±0.1%). An in vitro release research was carried out, and the results revealed that the chosen formula CLD released the entire amount of medication in 45 minutes, as opposed to just 19% for the pure drug. Ex vivo experiments revealed that F12 increased flow by approximately 4.2 times as compared to CLD suspensions.

Keywords: Cilnidipine, Nanomicelles, D-α-tocopherol, Polyethylene glycol 1000 succinate, Soluplus

#### Introduction

In order to increase the solubility and improve the stability and oral biological availability of poorly water-soluble compounds, several strategies have been suggested. One is using nanomicelles that have emerged as efficient tools for the encapsulation of drugs with low aqueous solubility [1-4]. The core—shell

Access this article online					
Website: www.japer.in	<b>E-ISSN</b> : 2249-3379				

**How to cite this article:** Tamer MA, Ali MM, Abbas IK, Ghareeb MM. Improving the dissolution rate of cilnidipine via nano-micellar formulation aided with *In-vitro* characterization and *Ex-vivo* permeation. J Adv Pharm Educ Res. 2025;15(4):75-83. https://doi.org/10.51847/1G3ULXpAon

structure of micelles prevents the penetration and presence of water in its inner core. This key feature of micelles creates a suitable environment for the encapsulated drug in comparison with the free drug [5]. Some advantages presented by micelles as drug carriers include easy development, affordable costs, facilitated transport of cargo across biological barriers, improved solubility in aqueous media including the unstirred water layer of the intestine, a controlled release profile, and protection against degradation [6]. The bioavailability of class II drugs and the desired clinical efficacy. Increased apparent solubility in water was achieved through the formulation of nano-micelles using large molecular weight molecules that self-assembled into vesicle-like structures with an outer hydrophilic shell and an inner lipophilic core [7, 8]. Cilnidipine is a BCS Class-II substance with a very low solubility and a high permeability [9]. CLD has an extremely low oral bioavailability in humans (13%). It also

This is an open access journal, and articles are distributed under the terms of the Creative Commons Attribution-Non Commercial-ShareAlike 4.0 License, which allows others to remix, tweak, and build upon the work non-commercially, as long as appropriate credit is given and the new creations are licensed under the identical terms.

exhibits low water solubility and slow dissolution [10]. CLD with half-life (2.5 h) [11]. Both L-type voltage-gated calcium channels in vascular smooth muscle and N-type calcium channels in sympathetic nerve terminals that supply the blood vessels are blocked by cilnidipine. Ceasing the activity of N-type calcium channels could potentially serve as a novel treatment strategy for cardiovascular disorders [12-15]. Administration of cilnidipine, which shows a reduction in cardiovascular outcomes, reduced the incidence of cardiovascular disease and target organ damage [16]. This research aims to enhance the oral bioavailability of cilnidipine by formulating it into a nano-micellar (NM) dosage form, thereby improving its dissolution rate.

#### Materials and Methods

CLD and TPGS were purchased from Hangzhou Hyper Chemicals Limited. SLP was purchased from BASF in Germany. Tween-80 and Poloxamer-188 were purchased from Fluka Chemical. Methanol was purchased from Loba Chemie Pvt. Ltd.,

India. Deionized water (DW) and the other chemicals and reagents were of analytical grade [17, 18].

#### Method of preparation of CLD -NM

Twenty mg of CLD was dissolved in 5 mL of an organic solvent (absolute methanol). The required quantities of each polymer (SLP, TPGS, Tween 80, and poloxamer 188) according to the specified ratios [(1:2), (1:4), (1:6), (1:8), (1:4:1), and (1:4:2)] were dissolved in 5 mL of the same organic solvent. Both solvents were mixed and stirred in a round-bottom flask over a magnetic stirrer at 45°C for 15 minutes. The solvent mixture was then evaporated for 10 minutes at 60 °C using a rotary evaporator (Bibby Scientific Limited - UK). Afterward, the flask was left overnight to allow any remaining solvent to drain. A magnetic stirrer at 300 rpm was used for two hours to hydrate the film by adding 10 mL of deionized water (DW) [19, 20].

**Table 1** shows that thirteen formulas were prepared, seven of which are single polymeric NM, and the others are mixed NM. All were subjected to *in-vitro* Characterization and evaluation.

NM C. 1.	CLD ()	D. D die	C-1 T	CI D ()	TDCC ()	TWN 90 ()	D-1- 100 ()	DW 4 - (1)
NM Code	CLD (mg)	D-P ratio	Solvent Type	SLP (mg)	TPGS (mg)	TWN 80 (mg)	Polo 188 (mg)	DW q.s to (ml)
F1	20	1:2	METH	40				10
F2	20	1:4	METH	80				10
F3	20	1:6	METH	120				10
F4	20	1:8	METH	160				10
F5	20	1:4	METH		80			10
F6	20	1:6	METH		120			10
F7	20	1:8	METH		180			10
F8	20	1:4:1	METH	80		20		10
F9	20	1:4:2	METH	80		40		10
F10	20	1:4:1	METH		80	20		10
F11	20	1:4:2	METH		80	40		10
F12	20	1:4:2	METH	80			40	10
F13	20	1:4:2	METH		80		40	10

### Characterization of CLD nano-micelles micelles size determination

The micelle size, polydispersity index (PDI), and zeta potential of the diluted formulation were determined using a Zetasizer (Malvern Instruments Ltd, United Kingdom) [21].

### Entrapment efficiency and drug loading capacity

Drug loading capacity (DL) and entrapment efficiency (EE) were computed indirectly. An ultrafiltration tube (Amicon MWCO

10000 D, Millipore Co., USA) was filled with a polymeric micelle dispersion, and the tubes were centrifuged for 30 minutes at 6000 rpm. Using the calibration curve for CLD in methanol and UV spectrophotometry with a wavelength of 242 nm, the amount of unincorporated CLD in the supernatant was measured. The unloaded CLD may be deducted from the first added CLD in order to get the loaded CLD quantity. The (EE%) and (DL%) were then computed using Eqs. 1 and 2 [22, 23]. This technique guarantees precise measurement of drug loading and encapsulation in nanomicellar systems.

$$\label{eq:eeg} \begin{split} \text{EE\%} &= \frac{\text{weight of drug encapsulated in micelle}}{\text{theoretical weight of Amisulpride added}} \\ &\quad \times 100 \end{split} \tag{1}$$

$$DL\% = \frac{\text{cweight of drug encapsulated in micelle}}{\text{Total weight of micelle (Amisulpride + polymer}} \times 100$$
 (2)

### Determination of the CLD solubility in different media

After adding an excess amount of CLD to a fixed volume of each PBS (pH 6.8), methanol, and distilled water, the mixture was incubated for 48 hours at 37°C in a shaking water bath to reach equilibrium. The suspension was centrifuged for 30 minutes at 6000 rpm and then passed through a 0.45  $\mu m$  pore membrane filter. The calibration curve of CLD in each of the media mentioned above was used to determine the concentration of CLD in the filtrate. The experiment was conducted in three duplicates, and the mean  $\pm SD$  was determined [22].

### In-vitro release of CLD from the prepared NM dispersion

The in-vitro release profile of CLD-loaded nano micelles (CLD-NMs) was evaluated using a dialysis membrane bag (cellulose membrane with a molecular weight cutoff of 8,000–14,000 Da) and phosphate-buffered saline (PBS at pH 6.8, containing 1% SLS) as the release medium. Before the experiment, the dialysis bag was soaked overnight in PBS (pH 6.8). Then, 2.5 mL of the CLD-NM dispersion, containing the equivalent of 5 mg of CLD, was placed inside the bag, as well as 2.5 mL containing only 5 mg of pure CLD drug suspended in DW. Each bag was then repeatedly submerged in 900 mL of release medium maintained at 37°C and stirred at 100 rpm using a USP dissolution apparatus type II, following the FDA's recommended dissolution protocol for CLD oral tablets. Samples of 5 ml were withdrawn at predetermined intervals (5, 10, 15, 30, 45, 60 min). An equal volume of fresh dissolution medium was replenished. The amount of CLD released was measured spectrophotometrically at 242 nm [24].

#### Selection of the optimum formula

The best formula was chosen based on the characterization's invitro results (particle size, PDI, EE%, and DL%), as well as the cumulative percentage released of CLD over 180 minutes. The proposed formula was further studied, including morphological determination using field-emission scanning electron microscopy (FESEM) and differential scanning calorimetry (DSC), to confirm that AMS was entrapped within the generated nanomaterial (NM). In addition, FTIR analysis was performed on the improved formula to ensure that the medication and excipient are compatible.

#### Ex-vivo intestinal absorption – non-everted

#### sac method

Ex-vivo investigations were performed using the non-everted intestinal sac technique on male Wistar rats weighing 250-300 g. The University of Baghdad's College of Pharmacy provided the animals for its animal house. The Research Ethics Committee of the University of Baghdad College of Pharmacy formally approved the study. The animal was sedated with ethyl ether, allowed to fast for the entire night with unfettered access to water, and had a 4 to 5 cm longitudinal abdominal incision performed. After removing the small intestine, the mesentery was manually scraped and then thoroughly cleaned out with cold normal saline solution using a blunt-ended syringe. One milliliter of the selected NM, containing two milligrams of medication, was placed in each of the equal-length, 10-cm-long sacs made from clean intestine, which were then knotted at the other end to form a sac [25]. Two milligrams of pure CLD powder suspended in 2.5 mL of deionized water (DW) was used as a control [26-29]. The duodenum was  $2.21 \pm 0.04$  mm in diameter [30]. At  $37^{\circ}$ C  $\pm$  2, the sac was submerged in 300 mL of phosphate-buffered saline solution (pH 7.4) after being attached to the paddle of a dissolution device type II. At intervals of 5, 10, 15, 30, 45, 60, 90, and 120 minutes, samples of a 5 mL solution were withdrawn and replaced with a phosphate-buffered saline solution (pH 7.4). Using a UV spectrophotometer and a calibration curve of CLD in phosphate-buffered saline (pH 7.4) at an absorption wavelength of 242 nm, the drug concentration in the aliquot portion was assessed. The research was carried out in triplicate, and the data was analyzed using the mean  $\pm$  SD. The permeability coefficient was determined using the following equations [31]:

$$PC = FSA \times C^{\circ}$$
 (3)

$$SA = 2\pi rh \tag{4}$$

The permeation flow (F) was calculated by calculating the slope of the linear section of the plot, where (r) represents the intestinal radius (cm) and (h) represents the intestinal segment length (cm). The flux reflects the permeability coefficient (PC, cm/min) (F,  $\mu g/min/cm^2$ ), intestinal sac area (SA, cm²), and initial drug concentration (Co).

#### Morphological characterization

Field emission scanning electron microscope(FESEM)

FESEM was utilized to study the morphology of the CLD nanomicelles formulation (FESEM S-4160, Hitachi, Japan). Sample preparation is an essential stage in the imaging of samples with a Field Emission Scanning Electron Microscope (FESEM). The quality of the sample preparation substantially determines the

quality of the pictures obtained from the FESEM. The sample preparation comprises carefully collecting nano-micelles to avoid contamination or damage, sample fixation in which the structural integrity of the formula is preserved, and dehydration of the formula to remove water from nano-micelles. Critical point drying is a technique used to remove the solvent from the formula without damaging the morphology of the nano-micelles. The formula is mounted on a stub using a conductive adhesive carbon tape and coated to prevent charging and improve image quality. The nano-micelles formula was coated with a conductive material, platinum, and finally imaged; the nano-micelles formula is now ready to be imaged using the FESEM [21].

#### Crystallinity specification

#### Differential scanning calorimetry (DSC)

The formulation was subjected to a DSC thermal analysis of the CLD, the physical mixture and the optimum CLD-NM formula. Under a flow of nitrogen gas, each sample was carefully weighed and stored in aluminum pans. Then, they were heated at a rate of  $10^{\circ}$ C/min and cooled at a rate of  $40^{\circ}$ C/min. In the research, an empty aluminum baking pan served as a control [32].

## Drug- excipient compatibility study Fourier transform infrared spectroscopy (FTIR)

FTIR spectroscopy in conjunction with the attenuated total reflectance (ATR) approach was utilized to detect any potential contact or complexation between the active ingredient and selected excipients, as well as AMS-excipient compatibility. CLD, in the form of mined powder with the selected CLD-NM formulae, was introduced directly into the crystal area without prior processing. The pressure arm was then placed above the sample and scanned throughout a wavelength range of 4000 - 400  $\rm cm^{-1}$  [33].

#### Statistical analysis

The results of the experiments are presented as the mean SD of triplicate models, and the significance of the observed changes in the applied components was determined using one-way analysis of variance (ANOVA) at the 0.05 level of significance [34].

#### Results and Discussion

### Effect of polymer type and concentration on the In-vitro characterization of ANM-NM

It is evident from the CLD-NM characterization results in **Table 2** that a direct decrease (significantly decreased P<0.05) in particle sizes (108.1  $\pm$  0.6, 85.28  $\pm$  0.4, 83.36  $\pm$  0.6, and 47.82

 $\pm$  0.4, respectively) is linked to increasing the concentration of SLP from 1:2, 1:4, 1:6, and 1:8. Particle size and PDI values are significantly impacted by SLP concentration as it rises from 0.4% w/v (F1) to 1.6% w/v. The hydrophobic tails of many surfactant molecules combine to form an oil-like core, which is a representation of the surfactant action of SLP and results in micelle characteristics. This core's most stable form made no touch with water. Because of its amphiphilic nature, SLP has been shown to form self-assembled spherical micelles in an aqueous environment above a CMC of 7.6 mg/L, with the polyethylene glycol backbone acting as the hydrophilic component and the vinyl caprolactam/vinyl acetate side chains acting as the lipophilic component. As a result, the solubility of poorly soluble medications can be greatly increased. In the current investigation, all SLP dispersion concentrations tested were over the CMC [35].

The PDI of the CLD-NM dispersion prepared with SLP is between 0.161±0.002 to 0.2387±0.001, which indicates the nano micelles are very uniform in size, with almost no variation between particles, i.e., a highly monodispersed system, which was very important to ensure predictable drug release and improve stability of the formulations [36].

The findings of particle size estimate for the formulations made with TPGS show that the average diameter of NM increases as the TPGS concentration increases. When the concentration of TPGS increases from 0.8% w/v (F1) to 1.6% w/v (F5 - F7), the influence on particle size is significant but not on PDI values. The same result was seen with SLP/TPGS silymarin nanomicelles; increasing the concentration of TPGS resulted in larger particle sizes [37]. **Figure 1** and **Table 2** show that EE% and DL% were measured for all of the prepared mixed polymeric NMs, ranging from F1 to F7, with no significant changes (P>0.05) and a high value for these two parameters.

### Effect of polymer combination on the invitro characterization of ANM-NM

Based on the in vitro characterization of the SLP-NM and TPGS -NM dispersions (F1 -F7), the drug-polymer ratio (1:4) was selected for the preparation of mixed polymeric NM via (1:4:1) and (1:4:2) ratios with SLP-TWN 80 (F8 and F9), TPGS-TWN 80 (F10 and F11), SLP- POL-188 (F12), and TPGS - POL-188 (F13), as declared in Figure 1 and Table 2 indicate that particle size, PDI, EE% and DL% were measured for all the prepared mixed polymeric NMs, showing no significant changes (P > 0.05) in EE%, and DL%, except for F10 and F13, which were excluded from this test due to their significant high particle size and PDI. The particle size of SLP/TWN 80 nanomicelles is smaller than that of SLP/TPGS. SLP has amphiphilic characteristics due to copolymer grafting. The backbone of polyethylene glycol stands in for the hydrophilic component, while the side chains of vinyl caprolactam and vinyl acetate represent the hydrophobic component. The hydrophobic segments of SLP constitute the central region of the micelle,

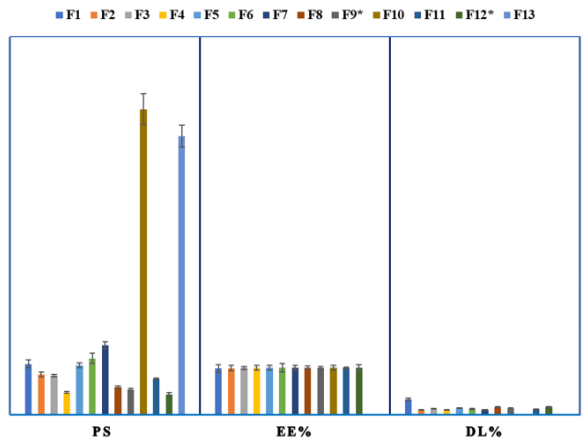
which acts as a microenvironment for the inclusion and integration of the lipophilic molecules. The inclusion of TPGS in nanomicelles has an adverse impact. This phenomenon is likely attributed to the fact that TPGS can reduce the hydrophobic contacts between the polymer chains within the micellar core [38]. If there is insufficient affinity between the drug and the copolymer within the core, the drug will not be effectively loaded into the micelle. As a result, the likelihood of interactions between hydrophilic and hydrophobic segments increases, causing changes in the hydrophobic nature of the core and, subsequently, affecting its ability to encapsulate the drug. This can clarify the phenomenon of particle size enlargement with increasing TPGS [39, 40]. Oral administration of nanomicelles

with an average hydrodynamic diameter below 100 nm can enhance intestinal medication absorption [37].

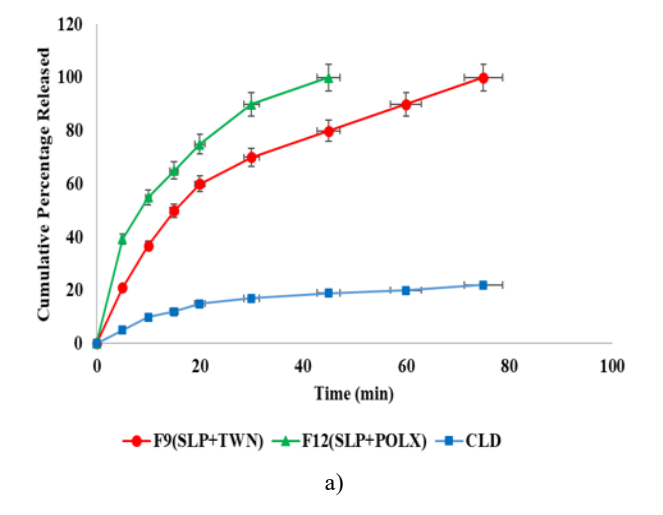
Micelles having particle sizes of 100 nm or smaller and acceptable technological parameters were chosen for further study. The particle size was reduced for F9 and F11, which were made using a drug-mixed polymeric ratio of 1:4:2, as compared to F8 and F10 with a ratio of 1:4:1, as shown in **Table 2** and **Figure 1**, so the ratio of 1:4:2 was chosen for further formulations. The effect of POL-188 as a copolymer was demonstrated in the measurement of particle size for F12, a nonionic surfactant with a reasonably high HLB that produced nanomicelles with the smallest size when compared to the other formulations [41].

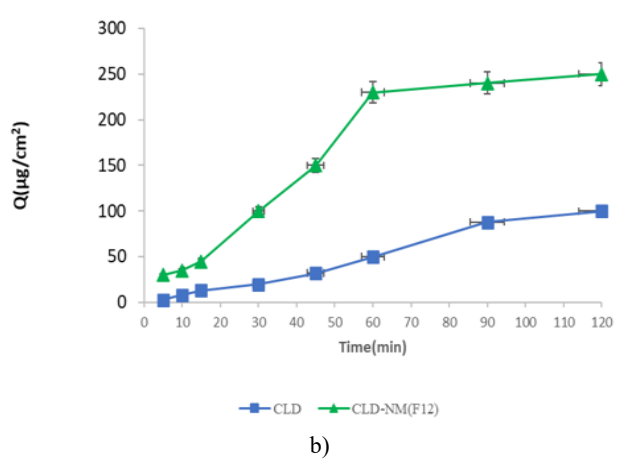
Table 2. *In-vitro* Characterization of CLD-NM (Particle size analysis, polydispersity index (PDI), entrapment efficiency (EE%), and drug loading (DL%).

NM Code	Drug-Polymer Ratio	Physical appearance	particle size (nm)	PDI	EE%	DL%
F1	1:2	Light Blue	$108.1 \pm 0.6$	0.2387 ±0.001	98 ±0.2	32.7±1.09
F2	1:4	Light Blue	$85.28 \pm 0.4$	0.161±0.002	98.8±0.1	10.99 ±0.09
F3	1:6	Light Blue	$83.36 \pm 0.6$	$0.2268 \pm 0.004$	99.6 ±0.1	13.81±0.89
F4	1:8	Light Blue	47.82 ±0.4	$0.2073 \pm 0.001$	99.8 ±0.25	11.04±1.3
F5	1:4	Light Blue	$105.3 \pm 0.8$	$0.3245 \pm 0.012$	99.4 ±0.2	14.21±.0.88
F6	1:6	Light Blue	$119.7 \pm 0.82$	$0.3599 \pm 0.13$	99.6 ±0.1	12.49±2.2
F7	1:8	Light Blue	$147.5 \pm 0.52$	$0.3869 \pm 0.04$	99.7±0.1	11.11±1.2
F8	1:4:1	Light Blue	$58.59 \pm 0.98$	$0.299 \pm 0.01$	98.6 ±0.2	16.67±0.99
F9*	1:4:2	Light Blue	$54.09 \pm 0.5$	$0.2688 \pm 0.28$	99.92±0.1	14.27±0.8
F10	1:4:1	Light Blue	646.8 ±0.95	$0.6658 \pm 0.01$		
F11	1:4:2	Light Blue	$76.68 \pm 0.5$	$0.4642 \pm 0.08$	90±0.5	12.9±0.6
F12*	1:4:2	Light Blue	43.76±0.3	0.2899±0.02	99.99±0.2	16.7±0.1
F13	1:4:2	Light Blue	$589.8 \pm 0.7$	$0.8871 \pm 0.12$		

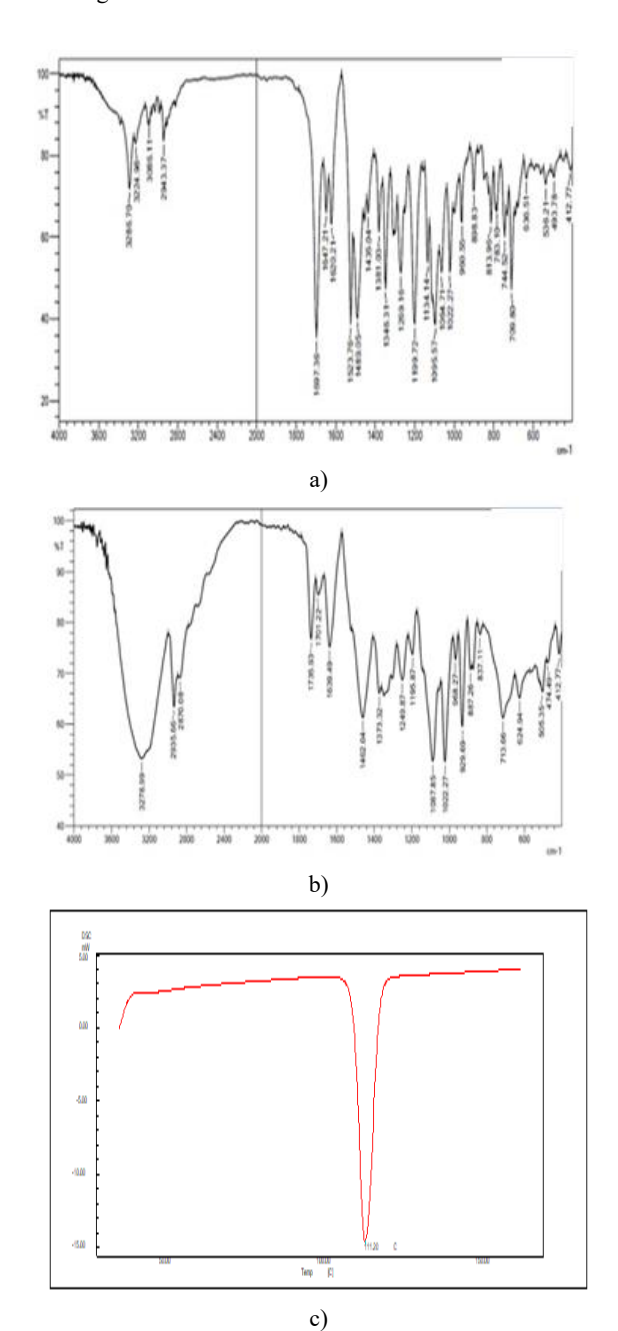


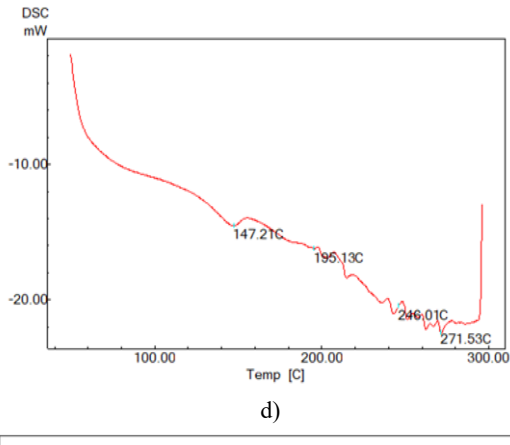
**Figure 1.** The Effect of polymer type, concentration and polymer combination on particle size, EE% and DL% (mean± SD, n=3).

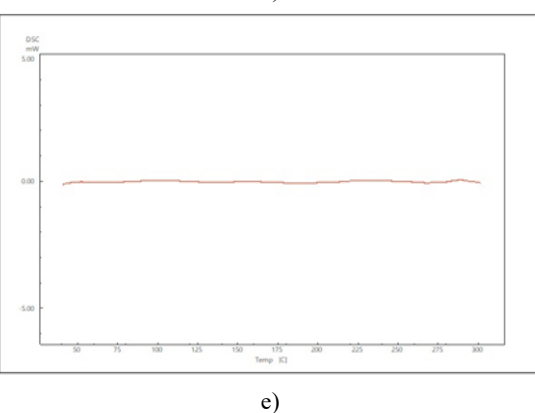




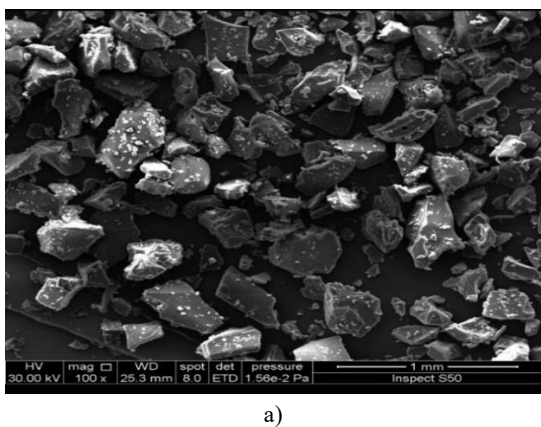
**Figure 2.** a) The release profile of CLD from F9, F12, and pure drug in PBS (pH 6.8) at 37°C, b) *Ex-vivo* intestinal absorption of CLD using the non-everted intestinal sac method







**Figure 3.** (a) FTIR spectra of CLD as a pure drug (b) FTIR spectra of CLD-NM (F12), (c) DSC thermogram of CLD, (d) DSC thermogram of physical mixture, (e) DSC thermogram of the selected formula (F12).



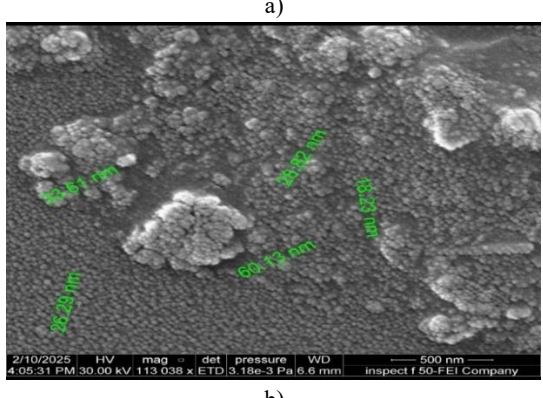


**Figure 4.** Field emission scan electron microscope of (a) Drug and (b) The optimized improved formula

### In-vitro release of CLD from the optimized CLD-NM dispersions

The release of CLD from NM containing Soluplus and Poloxamer (F12) is generally faster compared to NM formulated with Soluplus and Tween 80 (F9), as illustrated in Figure 2a. Which can be attributed to the differing physicochemical properties of the surfactants and polymers involved. Poloxamer (a nonionic triblock copolymer) tends to form micelles with relatively looser hydrophobic cores. It has thermoresponsive gelation properties, which can facilitate quicker drug diffusion and release from the NM matrix, while Tween 80 (a nonionic surfactant with a bulky hydrophilic head) often forms more stable and tighter micellar structures that can retard drug release, leading to a slower, more sustained release profile. Both formulas exhibit a significant improvement in the dissolution rate and extent of CLD. F12 achieves a 100% release, while F9 achieves an 80% release within 45 minutes, compared to the 19% release using an aqueous CLD drug suspension.

### Ex-vivo permeation of CLD from the optimized CLD-NM dispersions

Ex-vivo permeation studies were carried out using the noneverted intestinal sac technique. In comparison to the pure CLD aqueous suspension, Figure 4 illustrates that the total amount of CLD that penetrated the intestinal mucosa for F12 was almost 2.5 times greater, in which the flux and permeability coefficient of the selected formula were found to be 3.33± 0.006  $\mu g/cm2.min$  and 1.67±0.002 (cm/min) \*10  $^{\text{-}3}$  with a lag time of  $5\pm0.02$  min, while those of the pure drug were  $0.8\pm0.031$  $\mu g/cm^2$ .min and  $0.4\pm0.0028$  (cm/min) \*10<sup>-3</sup> with a lag time of 20±0.13 min, respectively. The flow and permeability coefficient values for F12 are significantly (p  $\leq 0.05$ ) higher than those for the pure CLD aqueous suspension, as shown in Figure 2b. Poor water solubility is the primary cause of CLD's restricted intestinal transfer; however, F12, which stands for CLDpolymeric NM, can increase the permeability of the drug by supplying a greater concentration gradient at the barrier interface as the drug dissolves at higher concentrations [42]. Furthermore, SLP has been observed to enhance the penetration of insoluble medications and inhibit the activity of the efflux pump [43]. These results could help clarify how CLD-NM can be utilized as a novel vehicle for poorly water-soluble medicinal compounds and how it can be used to enhance the degree of drug release and penetration, thereby increasing absorption and bioavailability.

#### Drug-polymer compatibility study

FTIR spectroscopy was utilized to evaluate potential chemical interactions between CLD and other excipients. **Figure 3b** shows the FTIR spectra of the selected NM (F12), which showed distinct CLD peaks. The majority of the CLD peaks were maintained, and there was no obvious change in wave number or

other notable disappearances in the spectrum, providing additional evidence that there were no discernible interactions between the functional groups of CLD and stabilizers, as well as strong compatibility between drugs and excipients [44, 45]. **Figure 3a** displays the FTIR spectra of pure CLD, with the observed values as: the absorption peaks of N-H stretching vibration were 3286 and 1697 cm<sup>-1</sup>, c=o stretching was 1701 cm<sup>-1</sup>, c=c stretching of aromatic was 1462 cm<sup>-1</sup>, NO<sub>2</sub> stretching were 1523 and 1346 cm<sup>-1</sup> and the O=CH3 deformation vibration and stretching were 1134 and 1623 cm<sup>-1</sup>.

**Figure 3c** shows that the bulk CLD has a prominent endothermic melting peak at 111.2°C, which can indicate the purity of the CLD powder examined. The DSC thermogram of the physical mixture of CLD as dipected by **Figure 3d** showed a melting point with an observed broadened peak, whereas the thermogram of the selected formula (F12\*) shown by **Figure 3e** was highly broadened with reduced intensity and sharpness, indicating that CLD was transformed to a highly amorphous state during the preparation of CLD nanomicelles [46, 47].

#### Field emission scan electron microscope

**Figure 4b** demonstrates that the optimized improved formula is spherical and with nano-sized particles compared with CLD powder that appears in **Figure 4a** as irregular macro-sized particles. The shape and size of the nanomicellar particles did not significantly alter as they accumulated those results were compatible with those reported by Sulaiman HT [12].

#### Conclusion

The NMs technique is a promising approach for addressing the challenges associated with the oral drug delivery system of poorly soluble drugs. The present study successfully incorporated cilnidipine into nanomicelles utilizing a thin film hydration technique. The cilnidipine nanomicelles offers a convenient and durable method of administering medication with a fast rate of drug dissolution.

Acknowledgments: The University of Baghdad's College of Pharmacy for providing the apparatus and the animals for achieving this study.

Conflict of interest: None

Financial support: None

Ethics statement: The Research Ethics Committee of the University of Baghdad College of Pharmacy formally approved the study.

#### References

 Turlaev MU, Shikhnebiev AA, Kardanova ZA, Rokhoev MM, Mutigullina KR, Zakiev RR, et al. The role of society

- and economy in advancing hirudotherapy in Russia. Int J Vet Res Allied Sci. 2022;2(1):37-43. doi:10.51847/UI6IyFGbqT
- Marian M, Shah R, Gashi B, Zhang S, Bhavnani K, Wartzack S, et al. The role of synovial fluid morphology in joint lubrication and function. Int J Vet Res Allied Sci. 2024;4(2):1-4. doi:10.51847/WXAMJiBFbr
- 3. Devi YR, Lourembam DS, Modak R, Shantibala T, Subharani S, Rajashekar Y. Differences in gut microbiota of healthy and tiger band disease-infected oak tasar silkworms (Antheraea proylei J.). Entomol Lett. 2023;3(1):18-27. doi:10.51847/sReC3NTiUx
- Anushree A, Ali MZ, Ahsan J. Cognitive impairments induced by acute arsenic exposure in drosophila melanogaster larvae. Entomol Lett. 2023;3(2):1-8. doi:10.51847/T2OLB4wjap
- Mobasheri M, Attar H, Rezayat Sorkhabadi SM, Khamesipour A, Jaafari MR. Solubilization behavior of polyene antibiotics in nanomicellar system: insights from molecular dynamics simulation of the amphotericin B and nystatin interactions with polysorbate 80. Molecules. 2015;21:E6. doi:10.3390/molecules21010006
- Shakeri A, Sahebkar A. Opinion paper: nanotechnology: a successful approach to improve oral bioavailability of phytochemicals. Recent Pat Drug Deliv Formul. 2016;10:4–6. doi:10.2174/1872211309666150611120724
- Pignatello R, Corsaro R. Polymeric nanomicelles of Soluplus® as a strategy for enhancing the solubility, bioavailability and efficacy of poorly soluble active compounds. Curr Nanomed. 2019;9(3):184-97.
- Li Y, Zhang T, Liu Q, He J. PEG-derivatized dualfunctional nanomicelles for improved cancer therapy. Front Pharmacol. 2019;10:808.
- Murugesan M, Sankaranarayanan V. Development and characterization of solid dispersion based orodispersible tablets of cilnidipine. Beni-Suef Univ J Basic Appl Sci. 2022;11(1):83.
- 10. Diwan R, Ravi PR, Pathare NS, Aggarwal V. Pharmacodynamic, pharmacokinetic and physical characterization of cilnidipine loaded solid lipid nanoparticles for oral delivery optimized using the principles of design of experiments. Colloids Surf B Biointerfaces. 2020;193:111073.
- 11. Tandel H, Raval K, Nayani A, Upadhay M. Preparation and evaluation of cilnidipine microemulsion. J Pharm Bioallied Sci. 2012;4(1):4-5.
- 12. Alharbi IS, Alharbi AS, Ansari SH. Public awareness and perceptions of orthodontic treatment with invisalign in Qassim, Saudi Arabia. Turk J Public Health Dent. 2022;2(1):13-8. doi:10.51847/DrpPRdrDrf
- 13. Menhadji P, Patel R, Asimakopoulou K, Quinn B, Khoshkhounejad G, Pasha P, et al. The influence of teledentistry on patient satisfaction and treatment results in Saudi Arabia during the Covid-19 Pandemic. Turk J Public

- Health Dent. 2024;4(1):36-43. doi:10.51847/elHXU4OUAa
- Burgt TVD, Mullaney T, Plasschaert A. Assessment of discoloration induced by root canal sealers and color alterations post-bleaching. Int J Dent Res Allied Sci. 2024;4(1):1-6. doi:10.51847/HibZikXbm5
- 15. Maneea ASB, Alqahtani AD, Alhazzaa AK, Albalawi AO, Alotaibi AK, Alanazi TF. Systematic review of the microbiological impact of sodium hypochlorite concentrations in endodontic treatment. Int J Dent Res Allied Sci. 2024;4(2):9-15. doi:10.51847/PH80PpWOX7
- Mahalingan K, Geethalakshmi A, Sah BK. Formulation and evaluation of floating tablet of cilnidipine as an antihypertensive agent. IjpprHuman. 2020;19(1):147-59.
- Patatou A, Iacovou N, Zaxaria P, Vasoglou M, Vasoglou G. Corticotomy-assisted orthodontics: biological basis and clinical applications. Ann Orthod Periodontics Spec. 2022;2:8-13. doi:10.51847/0qGERVSoQm
- Kulkarni S, Zope S, Suragimath G, Varma S, Kale A. The influence of female sex hormones on periodontal health: a regional awareness study. Ann Orthod Periodontics Spec. 2023;3:10-8. doi:10.51847/v4EFMh6WEf
- Pignatello R, Corsaro R, Bonaccorso A, Zingale E, Carbone C, Musumeci T. Soluplus® polymeric nanomicelles improve solubility of BCS-class II drugs. Drug Deliv Transl Res. 2022;12:1991–2006. doi:10.1007/s13346-022-01182-x
- Rajab NA, Jawad MS. Preparation and evaluation of rizatriptan benzoate loaded nanostructured lipid carrier using different surfactant/co-surfactant systems. Int J Drug Deliv Tech. 2023;13(1):120-6.
- Abdulqader AA, Sultan NA. Preparation and characterization of posaconazole as a nano-micelle using d-α-tocopheryl polyethylene glycol 1000 succinate (TPGS). Iraqi J Pharm Sci. 2023;32:26-32.
- Sulaiman HT, Rajab NA. Soluplus and Solutol HS-15 olmesartan medoxomil nanomicelle based oral fast dissolving film: in vitro and in vivo characterization. Farmacia. 2024;72(4):794-804.
- 23. Hashim AAJ, Rajab NA. Anastrozole loaded nanostructured lipid carriers: preparation and evaluation. Iraqi J Pharm Sci. 2021;30(2):185-95.
- 24. Al Hazzaa RA, Rajab NA. Cilnidipine nanocrystals: formulation and evaluation for optimization of solubility and dissolution rate. Iraqi J Pharm Sci. 2023;32(Suppl):127-35.
- Abed HN, Hussein AA. Ex-vivo absorption study of a novel dabigatran etexilate loaded nanostructured lipid carrier using non-everted intestinal sac model. Iraqi J Pharm Sci. 2019;28(2):37-45.
- Spirito FD, Iacono VJ, Alfredo I, Alessandra A, Sbordone L, Lanza A. Impact of COVID-19 awareness on periodontal disease prevention and management. Asian J Periodontics Orthod. 2022;2:16-26. doi:10.51847/t8D9TJGOCU

- Prada AM, Cicalău GIP, Ciavoi G. Resin infiltration for white-spot lesion management after orthodontic treatment. Asian J Periodontics Orthod. 2024;4:19-23. doi:10.51847/ZTuGEanCSV
- Kumar D, Gurunathan D, Jabin Z, Talal S. Comparative efficacy of aromatherapy and conscious sedation in pediatric dental anxiety management. Ann J Dent Med Assist. 2022;2(1):14-21. doi:10.51847/TVRFhVaiIQ
- Hackenberg B, Schlich M, Gouveris H, Seifen C, Matthias C, Campus G, et al. Perceived competence of dental students in managing medical emergencies: a cross-sectional study. Ann J Dent Med Assist. 2023;3(1):20-5. doi:10.51847/SINUqaRTG2
- 30. Kothari A, Rajagopalan P. The assembly of integrated rat intestinal-hepatocyte cultures. Bioeng Transl Med. 2020;5(1):e10146.
- 31. Bothiraja C, Pawar AP, Dama GY, Joshi PP, Shaikh KS. Novel solvent-free gelucire extract of *Plumbago zeylanica* using noneverted rat intestinal sac method for improved therapeutic efficacy of plumbagin. J Pharmacol Toxicol Methods. 2012;66(1):35–42.
- 32. Shekhar Dey N, Mukherjee B, Maji R, Sankar Satapathy B. Development of linker-conjugated nanosize lipid vesicles: A strategy for cell selective treatment in breast cancer. Curr Cancer Drug Targets. 2016;16(4):357-72.
- Kumar R, Puppala K, Lakshmi V. Optimization and solubilization study of nanoemulsion budesonide and constructing pseudo ternary phase diagram. Asian J Pharm Clin Res. 2019;12(1):551-3. doi:10.22159/ajpcr.2018.v12i1.28686
- 34. Jabir SA, Rajab NA. Lasmiditan nanoemulsion as intranasal in situ gel: Relative bioavailability study. J Adv Pharm Educ Res. 2024;14(4):99-104.
- 35. Al-Akayleh F, Zakari Z, Adwan S, Al-Remawi M. Preparation, characterization and ex-vivo human skin permeation of ibuprofen-soluplus polymeric nanomicelle. Int J Pharm Sci Res. 2021;12(5):2863-9.
- 36. Jassem NA, Abd Alhammid SN. Ex vivo permeability study and in vitro solubility characterization of oral Canagliflozin self-nanomicellizing solid dispersion using Soluplus as a nanocarrier. Acta Marisiensis Ser Med. 2024;70(2):42-9. doi:10.2478/amma-2024-0011
- 37. Piazzini V, D'Ambrosio M, Luceri C, Cinci L, Landucci E, Bilia AR, et al. Formulation of nanomicelles to improve the

- solubility and the oral absorption of silymarin. Molecules. 2019;24(9):1-20.
- 38. Bernabeu E, Gonzalez L, Cagel M, Gergic EP, Moretton MA, Chiappetta DA. Novel Soluplus®—TPGS mixed micelles for encapsulation of paclitaxel with enhanced in vitro cytotoxicity on breast and ovarian cancer cell lines. Colloid Surf B Biointerfaces. 2016;140(1):403—11.
- Butt AM, Mohd CI, Katas H, Witoonsaridsilp W, Benjakul R. *In vitro* characterization of Pluronic F127 and D-α-Tocopheryl Polyethylene Glycol 1000 Succinate mixed micelles as nanocarriers for targeted anticancer-drug delivery. J Nanomat. 2012;2012(2):1-11.
- 40. Meng X, Liu J, Yu X, Li J, Lu X, Shen T. Pluronic F127 and D-α-Tocopheryl Polyethylene Glycol Succinate (TPGS) mixed micelles for targeting drug delivery across the blood brain barrier. Sci Rep. 2017;7(2964):1-12.
- Woodhead JL, Hall CK. Encapsulation efficiency and micellar structure of solute-carrying block copolymer nanoparticles. Macromolecules. 2011;44(13):5443-51. doi:10.1021/ma102938g
- 42. González R, Peña MÁ, Torrado G. Formulation and Evaluation of Olmesartan Medoxomil tablets. Compounds. 2022;2(4):334-52.
- 43. Zi P, Zhang C, Ju C, Su Z, Bao Y, Gao J, et al. Solubility and bioavailability enhancement study of lopinavir solid dispersion matrixed with a polymeric surfactant-Soluplus. Eur J Pharm Sci. 2019;15(134):233-45.
- 44. Salih O, Muhammed E. Preparation, evaluation, and histopathological studies of ondansetron-loaded invasomes transdermal gel. J Res Pharm. 2024;28(1):289-303.
- 45. Tamer MA, Kassab HJ. The development of a brain targeted mucoadhesive amisulpride loaded nanostructured lipid carrier. Farmacia. 2023;71(5):1032-44.
- 46. Diwan R, Khan S, Ravi PR. Comparative study of cilnidipine loaded PLGA nanoparticles: process optimization by DoE, physico-chemical characterization and in vivo evaluation. Drug Deliv Transl Res. 2020;10(5):1442-58.
- 47. Kuhikar A, Khan S, Kharabe K, Singhavi D, Dahikar G. Improvement in aqueous solubility of cilnidipine by amorphous solid dispersion, its formulation into interpenetrating polymer network microparticles and optimization by Box-Behnken design. FABAD J Pharm Sci. 2021;46(1):1-12.